

Decoupling of Two Closely Located Dipole Antennas by a Split-Loop Resonator

Masoud Sharifian Mazraeh Mollaei, Anna Hurshkainen, Sergey Kurdjumov,
Stanislav Glybovski, Constantin Simovski

► **To cite this version:**

Masoud Sharifian Mazraeh Mollaei, Anna Hurshkainen, Sergey Kurdjumov, Stanislav Glybovski, Constantin Simovski. Decoupling of Two Closely Located Dipole Antennas by a Split-Loop Resonator. 2019. hal-01951312

HAL Id: hal-01951312

<https://hal-amu.archives-ouvertes.fr/hal-01951312>

Preprint submitted on 29 Jan 2019

HAL is a multi-disciplinary open access archive for the deposit and dissemination of scientific research documents, whether they are published or not. The documents may come from teaching and research institutions in France or abroad, or from public or private research centers.

L'archive ouverte pluridisciplinaire **HAL**, est destinée au dépôt et à la diffusion de documents scientifiques de niveau recherche, publiés ou non, émanant des établissements d'enseignement et de recherche français ou étrangers, des laboratoires publics ou privés.

Decoupling of Two Closely Located Dipole Antennas by a Split-Loop Resonator

Masoud Sharifian Mazraeh Mollaei, Anna Hurshkainen, Sergey Kurdjumov, Stanislav Glybovski and Constantin Simovski

Abstract—In this letter, we theoretically and experimentally prove the possibility of the complete passive decoupling for two parallel resonant dipoles by a split-loop resonator. Unlike previously achieved decoupling by a similar resonant dipole, this decoupling technique allows us to avoid the shrink of the operation band. Compare to previous work, simulation and measurement show 100% enhancement of relative operation band from 0.2% to 0.4%.

Index Terms—Antenna Array, Decoupling, Shared Impedance, Mutual Impedance.

I. INTRODUCTION

In many radio-frequency applications, antenna arrays consist of closely located dipoles and their decoupling is required. When the straightforward methods of decoupling (screens or absorbing sheets) are not applicable, one often uses adaptive technique when the decoupling is achieved involving active circuitry – operational amplifiers. However, in multi-input multi-output (MIMO) systems and antenna arrays for magnetic resonance imaging (MRI) the passive decoupling is preferred [1]–[6]. The keenest situation corresponds to compact arrays when the distance d between two parallel dipole antennas is smaller than $\lambda/10$, where λ is the wavelength in the operation band. Then, this gap is not sufficient in order to introduce an electromagnetic band-gap (EBG) structure or to engineer a defect ground state [1]–[3]. For passive decoupling of the loop antennas used in MRI radio-frequency coils one found specific technical solutions working for densely packed arrays (see e.g. in [4]). As to dipole arrays, the passive decoupling is realized either involving the strongly miniaturized (and challenging in its tuning) EBG structures [5] or arrays of passive scatterers [6]. However, in both these cases the success was achieved when $d \approx \lambda/12$, whereas there is a strong need in dipole antenna arrays arranged with $d < \lambda/30$ [1], [7].

A complete passive decoupling of two resonant dipole antennas 1 and 2 separated by an arbitrary gap d (the minimal value of d is restricted only by the requirement $d \gg r_0$, where r_0 is the wire cross section radius) was suggested and studied theoretically and experimentally in [8]. The decoupling is achieved by placing a similar resonant but passive dipole 3 (half-wave straight wire) in the middle of the gap. Then the electromotive force (EMF) induced by dipole 1 in dipole 2 is compensated by a part of the electromotive force induced in dipole 2 by scatterer 3. Similarly, scatterer 3 when excited

by dipole 2 compensates the EMF induced by dipole 2 in dipole 1. This decoupling is complete, meaning that the power flux from dipole 1 to dipole 2 (and vice versa) is substituted by the flux from these dipoles to the scatterer for whatever relations between currents in dipoles 1 and 2. They both can be active, one of them can be active whereas the other can be loaded at the center by a lumped load or can be shortcut, they remain decoupled. However, this decoupling is approximate in the meaning that the power flux between dipoles 1 and 2 is suppressed not completely. For practical applications it is enough to reduce the mutual power transmittance by 10-12 dB. However, the bandwidth of antennas may suffer of the presence of scatterer 3. This is the case of [8], when the band of the resonant lossless matching (when the antenna circuits are tuned at the decoupling frequency) shrunk seven times due to passive dipole 3; and the bandwidth of the decoupling regime was as narrow as the resonance band.

The purpose of the present study is to find a decoupling scatterer for two dipole antennas separated by a gap $d < \lambda/30$ as compact and efficient as the half-wave straight wire but more broadband. We will show that it can be achieved using an elongated split loop resonating at the same frequency as dipoles 1 and 2. We called such the loop (depicted in Fig. 1) split-loop resonator (SLR).

II. THEORY OF DECOUPLING BY A SPLIT-LOOP RESONATOR

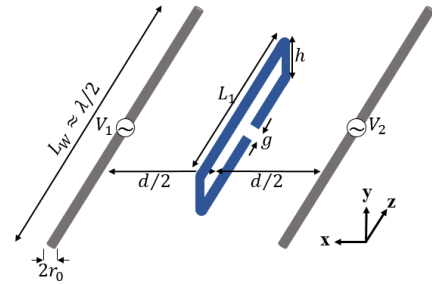


Fig. 1. A resonant SLR 3 located in the middle between antennas 1 and 2.

Now let us prove that decoupling of dipoles 1 and 2 located in free space is possible with an SLR symmetrically located between them. Since the loop contour C comprises the gap g we may consider the SLR as a wire scatterer. The method of induced EMFs is applicable to our SLR, as well as it was applicable to the dipole of our previous work [8]. Therefore, the condition of the complete decoupling expressed by formula (12) of work [8]

$$Z_{13}^2 = ZZ_M \quad (1)$$

M. S. M. Mollaei and C. Simovski are with Aalto University, FI-00076 Espoo, Finland

A. Hurshkainen, S. Kurdjumov and S. Glybovski are with ITMO University, 197101 St. Petersburg, Russia

remains valid for the structure depicted in Fig. 1. Here Z_M is mutual impedance between dipoles 1 and 2, Z is the self-impedance of our SLR, and $Z_{13} = Z_{23}$ is its mutual impedance with antenna 1 or antenna 2. Both Z and Z_M are referred to the scatterer center – reference section (RS) located on the solid (top) side of the loop as shown in Fig. 2.

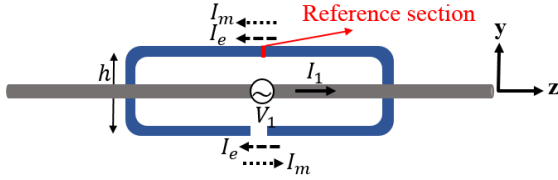


Fig. 2. The side view of the structure comprising an active dipole 1 driven by an external voltage V_1 and the passive SLR 3. Current I_3 induced in the SLR is the sum of the electric I_e and magnetic I_m modes. At $(y = +h/2, z = 0)$ $I_m = I_e = I_0/2$, at $(y = -h/2, z = 0)$ $I_m = -I_e = -I_0/2$.

In Fig. 2 we depict the side view of our structure. A primary source V_1 in the center of dipole 1 induces in our SLR 3 two current modes – an electric one I_e symmetric and an antisymmetric magnetic one I_m with respect to the plane $y = 0$. If the current in the reference section of the SLR i.e. at point $(y = +h/2, z = 0)$ is denoted as I_0 both modes have the same amplitude $I_0/2$ at this point, whereas they mutually cancel each other at the gap that can be approximated by point $(z = 0, y = -h/2)$. The distribution of the electric dipole mode along the SLR is similar to that in a straight wire and, therefore, can be approximated as (see e.g. in [9]):

$$f_e(z) \equiv \frac{I_e(z)}{I_0/2} = \frac{\sin k \left(\frac{L_l}{2} - |z| \right)}{\sin \frac{kL_l}{2}}. \quad (2)$$

Contrary to the electric mode, the magnetic one is maximal at the vertical sides of the loop. This is so because these sides are shortcuts if our SLR is considered as a two-wire line. This model of the loop results in the following approximation:

$$f_m(z) \equiv \frac{I_m(z)}{I_0/2} = \pm \frac{\cos k \left(\frac{L_l}{2} - |z| \right)}{\cos \frac{kL_l}{2}}. \quad (3)$$

Sign plus corresponds to the top side of the loop ($y = +h/2$), sign minus – to the bottom side ($y = -h/2$).

Let us calculate the mutual impedance Z_{13} between dipole 1 and SLR 3 applying the general formula of the induced EMF method:

$$Z_{13} = \frac{1}{I_1} \int_C E_{13}(l) f_3(l) dl, \quad (4)$$

where I_1 is the current at the center of dipole 1, $E_{13}(l)$ is the tangential component of the electric field produced by this primary current at a point l of the wire contour C of scatterer 3, and $f_3(l) = f_e(l) + f_m(l)$ is the current distribution in scatterer 3. Decomposition of the current induced in 3 onto the electric and magnetic modes allows us to split the right-hand side of (4) into electric and magnetic mutual impedances

formed by the coupling of the primary current I_1 with the electric and magnetic modes, respectively. The antisymmetry of the magnetic mode results in two mutually cancelling EMFs induced in the top ($y = +h/2$) and bottom ($y = -h/2$) sides. In the vertical sides $E_{13} = 0$. Meanwhile, the equivalent EMFs corresponding to the electric mode sum up and (4) is simplified to

$$Z_{13} = \frac{2}{I_1} \int_{-L_l/2}^{L_l/2} E_{13}(z, y = \frac{h}{2}) f_e(z) dz. \quad (5)$$

This formula describes the mutual impedance of two effective dipoles one of which is dipole 1 length L_w , and the other one is one half of the SLR, e. g. its top side L_l . The problem of Z_{13} yields to the symmetric mutual coupling of two parallel dipoles of different lengths.

Formulas for the mutual impedance of two parallel and symmetrically arranged dipoles are known. We will use the integral formula of [11] which allows us to rewrite (5) as

$$Z_{13} = \frac{\eta}{2\pi} \int_{-L_l/2}^{L_l/2} f_e(z) F(z, \delta) dz. \quad (6)$$

Here $\eta = 120\pi$ Ohm is free space impedance and it is denoted

$$F(z, \delta) = \frac{e^{-jkr_+}}{r_+} + \frac{e^{-jkr_-}}{r_-} - 2 \cos \frac{kL_w}{2} \frac{e^{-jkr}}{r},$$

$r = \sqrt{z^2 + \delta^2}$, $\delta = \sqrt{(h/2)^2 + (d/2)^2}$, and values r_+ and r_- are distances from two ends of dipole 1 to the integration point:

$$r_- = \sqrt{\left(\frac{L_w}{2} - z \right)^2 + \delta^2}, \quad r_+ = \sqrt{\left(\frac{L_w}{2} + z \right)^2 + \delta^2}.$$

The result of the integration in (6) can be presented in the closed form even in the present case $L_l \neq L_w$ (see e.g. in [10]). However, all known representations of this result are too cumbersome. We will obtain a simpler expression for Z_{13} suitable for our purpose.

Namely, let us assume that both dipole 1 and SLR 3 resonate at the same frequency and the decoupling holds in their resonance band. The resonance of dipole 1 holds when $L_w \approx 0.496\lambda$ and in our SLR the loop inductance resonates with its capacitance. Assuming the capacitance of the gap g to be negligibly small (that is correct if $r_0 \ll g \ll L_l$) we may calculate the inductance of our rectangular loop using formulas of [12], and its capacitance – using formulas of [13]. Choosing as an example $L_w = 500$ mm and $r_0 = 1$ mm (then the resonance band of dipoles 1 and 2 centered by the resonance frequency can be specified as 290-310 MHz) we fit the resonance band of the SLR to that of the dipoles when $h = 10$ mm and $L_l = 290$ mm.

Since in this case L_l is noticeably smaller than $\lambda/2$, the sinusoidal current distribution (2) can be replaced by its quadratic approximation $f_e(z) = 1 - (2z/L_l)^2$. This formula seems to be rough, but it is even more accurate (at least when $L_l < \lambda/3$) than the commonly adopted sinusoidal approximation (2) which is not smooth at $z = 0$. Substitution

of the quadratic approximation into (6) and variable exchanges $L_l/2 \pm z \rightarrow \xi$ yield the right-hand side of this relation to a linear combination of following integrals:

$$J_1 = \int_{-\frac{L_l}{2}}^{\frac{L_l}{2}} \frac{e^{-jk\sqrt{\xi^2+a^2}}}{\sqrt{\xi^2+a^2}} d\xi,$$

$$J_2 = \int_{-\frac{L_l}{2}}^{\frac{L_l}{2}} \xi \frac{e^{-jk\sqrt{\xi^2+a^2}}}{\sqrt{\xi^2+a^2}} d\xi,$$

and

$$J_3 = \int_{-\frac{L_l}{2}}^{\frac{L_l}{2}} \xi^2 \frac{e^{-jk\sqrt{\xi^2+a^2}}}{\sqrt{\xi^2+a^2}} d\xi,$$

where a is a constant independent on ξ . Integrals of types J_{1-3} were calculated using the simplest variant of the stationary phase formula (see e.g. in [14]). In all these integrals the stationary phase point ξ centers the integration interval, whereas the contributions of the ends of this interval (points $\xi = \pm L_l/2$) cancel out in the final expression. This is not surprising because the dipole mode current nullifies at the edges of the SLR.

The stationary phase method is adequate because L_w is large enough and function $F(z)$ is oscillating. Skipping all involved but very simple algebra, the result takes form:

$$Z_{13} \approx \frac{\eta L_l}{3\pi} \left[\frac{kL_w e^{-jk\delta}}{4\sqrt{2\pi}\delta} - \cos \frac{kL_w}{2} \frac{kL_w e^{-jk\Delta}}{2\sqrt{2\pi}\Delta} \right]. \quad (7)$$

Here it is denoted $\Delta = \sqrt{(L_w/2)^2 + \delta^2}$. Further simplification results from the resonant length of our dipoles $kL_w = \pi$. The term with Δ in (7) vanishes and we obtain:

$$Z_{13} \approx \frac{\eta L_l e^{-jk\delta}}{24\sqrt{2\pi}\delta}. \quad (8)$$

Now, let us calculate the input impedance Z of an individual SLR entering (1). At frequencies near the resonance where the reactance is negligibly small, the input impedance is equal (neglecting the Ohmic losses) to the radiation resistance R_{SLR} . This radiation resistance is a simple sum of R_{el} – that of a Hertzian dipole with effective length L_{eff} (see e.g. in [9])

$$R_{el} = \frac{\eta}{6\pi} (kL_{eff})^2 \quad (9)$$

and R_{mag} – that of a magnetic dipole with effective area S_{eff} (see e.g. in [9])

$$R_{mag} = \frac{8\pi\eta}{3} (k^2 S_{eff})^2. \quad (10)$$

Parameters L_{eff} characterizing the distribution of the electric mode and S_{eff} (magnetic mode) are easily found via simple integration of f_e and f_m that gives in our example case $L_{eff} \approx L_l$ and $S_{eff} \approx L_l h$. Then, (9) and (10) for our example case give the radiation resistance of the resonant SLR $R_{SLR} = R_{el} + R_{mag} \approx 70$ Ohm. The resonant impedance of a half-wave dipole is also nearly equal $R_0 = 70$ Ohms [9]. Therefore, it is reasonable to assume that the input impedance Z of an

individual SLR at frequencies near its resonance is practically equal to that of the resonant dipole and can be approximated as $Z \approx R_0(1 + \beta\gamma)$, where $\beta \approx 59$ and $\gamma = (\omega - \omega_0)/\omega_0$ is relative detuning [8]. Substituting this approximation for Z , (8) for Z_{13} and (14a) of [8] $Z_M \approx (\eta/24\pi kd) \exp(-jkd)$ into (1), we obtain the decoupling condition as

$$\frac{R_0\eta}{24\pi kd} e^{-jkd}(1 + \beta\gamma) = \left(\frac{\eta L_l}{24} \right)^2 \frac{e^{-2jk\delta}}{2\pi\delta^2}. \quad (11)$$

In the case $h \ll d \approx d/2$ and complex exponentials cancel out that reduces (11) to the simplest equation from which we find the detuning γ corresponding to the decoupling

$$\beta\gamma = (\eta k L_l^2 / d R_0) - 1. \quad (12)$$

For $d = 3$ cm (in this case $h = d/3$) and $L_l = 29$ cm (12) yields $\gamma \approx 0.0423$ that implies the decoupling at the upper edge of the resonance band – at 312.8 MHz. Of course, this is an approximate decoupling, however, in our terminology it is complete since should be observed for whatever relations of currents in the active dipoles.

III. VALIDATION OF THE THEORY AND DISCUSSION

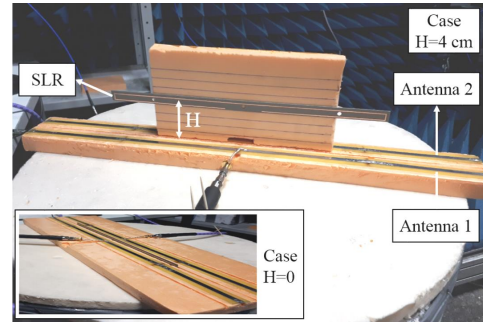


Fig. 3. Picture of the setup. The structure is supported by foam wrapped by paper. Slots in the vertical foam sheet show the height H of the SLR over the plane $y = 0$. The complete decoupling corresponds to $H = 0$.

Numerical investigations of S_{12} parameter calculated using CST Studio for dipoles 1 and 2 performed of a copper wire in absence and in presence of ideal matching circuits tuned at the frequency of decoupling. Simulations were done in absence of our SLR (reference structure) and in its presence. The decoupling frequency was taken exactly equal to that predicted by our theory (312.8 MHz) and the geometric parameters offering the decoupling at these frequency turned out to be surprisingly close to those predicted by our theory. Namely, for $d = 3$ cm the complete decoupling at frequency 312.8 MHz is achieved with following design parameters of antennas and SLR: $r_0 = 1$ mm, $L_l = 290.2$ mm, $L_w = 500$ mm, $h = 7$ mm. Also, in these simulations we took $g = 30$ mm that is not specified by the theory but satisfies its assumption $r_0 \ll g \ll L_l$. Simulations have confirmed our expectations about a broader band of both resonant matching and decoupling granted by an SLR compared to a resonant dipole [8]. The replacement of the decoupling dipole with an SLR enlarges the operation band from 0.2% [8] to 0.4%.

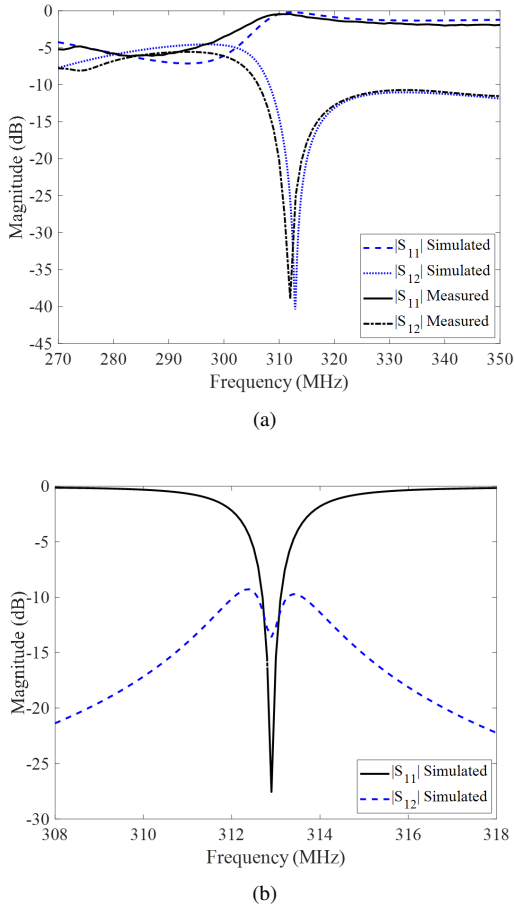


Fig. 4. Frequency dependencies of S_{11} and S_{12} for the system of our dipoles 1 and 2 decoupled by our SLR 3. (a) Mismatched case, (b) matched case.

For further validation we built an experimental setup pictured in Fig. 3. The setup is similar to that described in [8]. The main difference is the replacement of a straight wire by an SLR. Similar to [8], in this experiment we varied the height H of our SLR over the plane of the dipoles $y = 0$ ($H = 0$ corresponds to the initial location of the SLR centered by this plane). Note that our model developed above does not prohibit the decoupling in the case when $H \neq 0$ and the magnetic mode is induced in the SLR. However, both CST simulations and this experiment have shown no complete decoupling for $H \neq 0$.

Our experimental and numerical results are presented in Fig. 4. In both mismatched and matched regimes (Figs. 4(a) and 4(b), respectively), minima of S_{12} were simulated at 312.8 MHz that is the indication of the complete decoupling. Due to the difficulty of the tunable matching circuit, we measured the S-parameters only for the mismatched structure. Our measurements agree very well with simulations and can be considered as a confirmation of the theory.

Our simulations for the matched case show that the insertion of SLR 3 decreases S_{12} at 312.8 MHz by 10 dB (from -4 dB corresponding to the reference structure [8] to -14 dB). This is probably sufficient for many applications. The operational band of the decoupled system can be defined as the minimal one of two bands – that of the matching (the band where

$S_{11} \leq -15$ dB using a lossless matching circuit) and that of the decoupling (the band where $S_{12} \leq -10$ dB). In these definitions both bands of the matching and decoupling are equal to 1.3 MHz. This band is much wider than that offered by a decoupling dipole in [8] and this broadening is the main practical result. It follows from the fact that the extra mismatch due to the presence of the SLR at the distance $d/2$ from our antennas is not as high as the extra mismatch due to the presence of the dipole scatterer. We have not compared the simulation results of decoupling by passive SLR and dipole because the decoupling frequency is not the same for these cases; however, the enhancement of operating band is clear from comparison of S_{11} in Fig. 4(a) with S_{11} in Fig. 3 of paper [8].

IV. CONCLUSION

In this Letter, we have theoretically and experimentally shown the complete (for whatever ratio of source voltages and currents) decoupling of two very closely located resonant dipoles is possible by adding a passive scatterer different from the similar dipole studied in our previous work. Decoupling can be granted by an elongated split loop, having the resonance in the same frequency band as the dipole antennas. The usefulness of this technical solution is the enlarged operation band. Also, this study opens the door to further search of decoupling scatterers.

REFERENCES

- [1] H. Li, "Decoupling and Evaluation of Multiple Antenna Systems in Compact MIMO Terminals," Ph.D. dissertation, Dept. Elect. Eng., KTH Univ., Stockholm, Sweden, 2012.
- [2] Q. Li, "Miniaturized DGS and EBG structures for decoupling multiple antennas on compact wireless terminals," Ph.D. dissertation, Dept. Elect. Eng., Loughborough Univ., Loughborough, UK, 2012.
- [3] S. M. Wang, L. T. Hwang, C. J. Lee, C. Y. Hsu, and F. S. Chang, "MIMO antenna design with built-in decoupling mechanism for WLAN dual-band applications," *Electronics Lett.*, vol. 51, no. 13, pp. 966–968, June. 2015.
- [4] N. I. Avdievich, J. W. Pan and H. P. Hetherington, "Resonant inductive decoupling (RID) for transceiver arrays to compensate for both reactive and resistive components of the mutual impedance," *NMR Biomed.*, vol. 26, 1547-1554, Nov. 2016.
- [5] A. A. Hurshkainen, T. A. Derzhavskaya, S. B. Glybovski, I. J. Voogt, I. V. Melchakova, C. A. T. van den Berg, and A. J. E. Raaijmakers, "Element decoupling of 7 T dipole body arrays by EBG metasurface structures: Experimental verification," *J. Magn. Res.*, vol. 269, pp. 87–96, Aug. 2016.
- [6] E. Georget, M. Luong, A. Vignaud, E. Giacomini, E. Chazel, G. Ferrand, A. Amadon, F. Mauconduit, S. Enoch, G. Tayeb, N. Bonod, C. Poupon, and R. Abdeddaim, "Stacked Magnetic Resonators for MRI RF Coils Decoupling," *J. Magn. Res.*, vol. 175, pp. 11–18, Nov. 2016.
- [7] F. Padorno, A. Beqiri, J. V. Hajnal, S. J. Malik, "Parallel transmission for ultrahigh-field imaging," *NMR Biomed.* **29**(9), 1145-1161, 2016.
- [8] M. S. M. Mollaei, A. Hurshkainen, S. Glybovski, and C. Simovski, "Passive decoupling of two closely located dipole antennas," submitted to *IEEE Trans. Antennas Propag.*, available in arXiv:1802.07500.
- [9] C. A. Balanis, *Antenna Theory: Analysis and Design*, 4th Edition, NY, 2016.
- [10] R. S. Elliot, *Antenna Theory and Design*, Prentice Hall, NY, 1981, p. 225.
- [11] R.W.P. King, G.J. Fikioris, and R.B. Mack, *Cylindrical Antennas and Arrays*, Cambridge University Press, Cambridge, 2002, p. 160.
- [12] P.L. Kalantarov and A.A. Tseitlin, *Calculation of inductances*, Energoatomizdat, Leningrad, 1986, p. 187 (in Russian).
- [13] Yu.Ya. Yossel, E.S. Kachanov, and M.G. Strunski, *Calculation of electric capacitance*, Energoizdat, Moscow, 1981, p. 212 (in Russian).
- [14] N. Bleistein and R. Handelsman, *Asymptotic Expansions of Integrals*, Dover, NY, 1975, p. 36.